

## Supporting Information of

### Polymeric Micro-fabricated TiO<sub>2</sub>-ZrO<sub>2</sub> Affinity Chromatography Microchip for Phosphopeptide Enrichment and Separation

Katerina Tsougeni <sup>a</sup>, Panagiotis Zerefos <sup>b</sup>, Angeliki Tserepi <sup>a</sup>, Antonia Vlahou <sup>b</sup>,  
Spiros D. Garbis <sup>b</sup>, Evangelos Gogolides <sup>a\*</sup>

<sup>a</sup> *Institute of Microelectronics, NCSR “Demokritos”, PO BOX 60228, 153 10 Aghia Paraskevi, Greece*

<sup>b</sup> *Center of Basic Research-Division of Biotechnology, Biomedical Research Foundation, Academy of Athens, 11527 Athens, Greece*

#### 1. Information about Tryptone enzymatic digest from $\beta$ -Casein

Table S1a. Molecular weight distribution of Tryptone enzymatic digest from  $\beta$ -Casein

Molecular weight distribution	g / 100g
> 10000 Da	0
1000 – 10000 Da	8.2
500 – 1000 Da	23.0
300 – 500 Da	37.1
< 300 Da	31.7
<b>Average Molecular Weight</b>	<b>490 Da</b>

Table S1b. Quantity and pKa values of total and free amino acids contained in Tryptone enzymatic digest from  $\beta$ -Casein. Only the most abundant free amino-acids are listed

Amino-acids	Total (g/100g)	Free (g/100g)	pKa
Leucine	7.1	3.5	2.33
Lysine	5.7	3.1	2.16
Arginine	3.2	3.0	1.82
Phenylalanine	4.0	2.5	2.20
Tryptophan	1.2	1.2	2.46
Valine	4.7	0.9	2.39

Glutamic acid	18.1	0.4	2.10
<b>Total amino-acids</b>	<b>81.6</b>	<b>18.4</b>	-

## 2. Microchip Fabrication

First, a thin negative-tone inorganic–organic hybrid photoresist (ORMOCER) was spin-coated on the PMMA sheets (Thick Organic Photoresists, such as maP-1275<sup>®</sup> could also be used). Second, the thin Si containing polymer layer (~ 4µm) was exposed for 12 s through a photo-mask using UV broadband light 365-nm, and then baked at 80 °C for 4 min to induce crosslinking of the film. Third, the soluble unexposed part of Si containing polymer was removed (developed) for 1 min in MIBK (methyl-isobutyl-ketone) and IPA (iso-propyl-alcohol). Fourth, deep O<sub>2</sub> plasma etching of the PMMA substrates followed for 10 min under the following anisotropic conditions: -100V, 0.75Pa, 1900W, 100 sccm, -20°C.

## 3. Details of the UV-sensitive Peltier-cooled detection setup

The setup included: a) a light source with two lamps operated separately or simultaneously: DT-MINI-2-GS deuterium lamp from Ocean Optics, for the ultraviolet region (emitting from 200 to 410 nm), and a tungsten lamp from Ocean Optics (emitting 360 to 2000 nm) for the visible region. b) a spectrophotometer model QE65000-ABS from Ocean Optics containing a monochromator and a CCD detector model S7031-1006 from Hamamatsu (Sensitivity ~0.065 counts/e-, Signal to noise ratio (at full signal) 1000:1). The monochromator had a 50µm slit, and a Grating HC1-QE (300 lines/groove composite blaze, 200 nm – 950 nm range). The optical fibers used had the following specifications: QP200-2-SR-BX, 200µm core, Premium grade Solarization-Resistant High-OH content fiber, 200 – 1100 nm wavelength range, 2m long, with Stainless-steel BX jacket. The deuterium lamp presented low frequency baseline shifts of several milli absorbance units (mAU) which however did not mask the separation peaks.

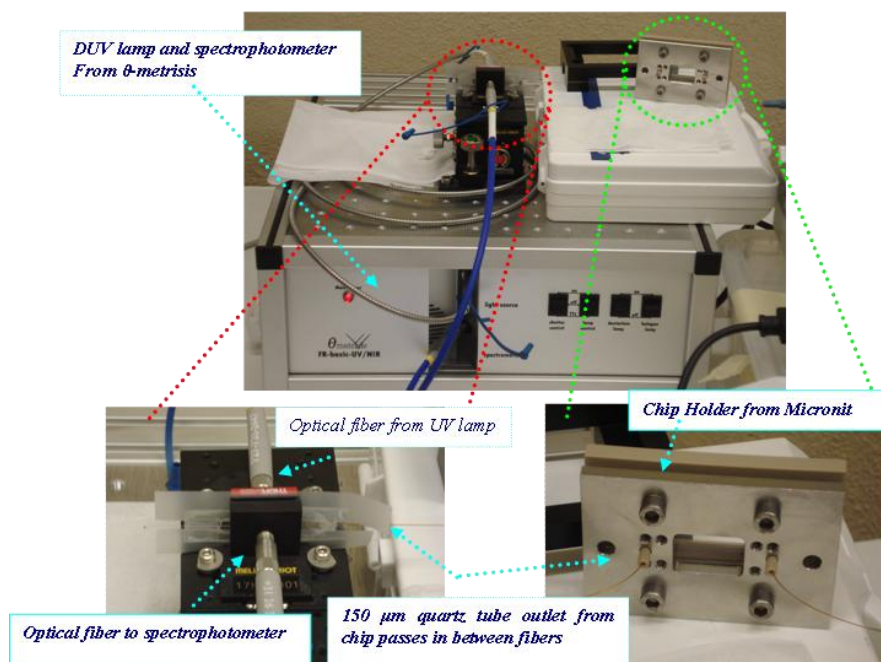


**Fig. S1** The microchip connected to detection setup. The area where the optical fiber is aligned with the quartz tube and the device holder are shown in enlargement.

#### 4. XRD spectra of liquid $\text{TiO}_2\text{-ZrO}_2$ deposition

Since it was difficult to acquire the XRD spectrum of  $\text{TiO}_2\text{-ZrO}_2$  film directly from the PMMA micro-column, an open PMMA surface was used. However to make sure that the surface has the same hydrophilicity, a mild oxygen plasma treatment was performed prior to deposition (RIE, 100 mT pressure, 100 W power, 10 min, 50 sccm oxygen flow rate).

The XRD spectrum shows peaks of the crystalline structure of  $\text{TiO}_2$  and  $\text{ZrO}_2$ . The first peak at  $25^\circ$  corresponds to the crystalline anatase form of  $\text{TiO}_2$  in direction (101) and the second peak at  $31^\circ$  corresponds to monoclinic  $\text{ZrO}_2$  system in direction (012).

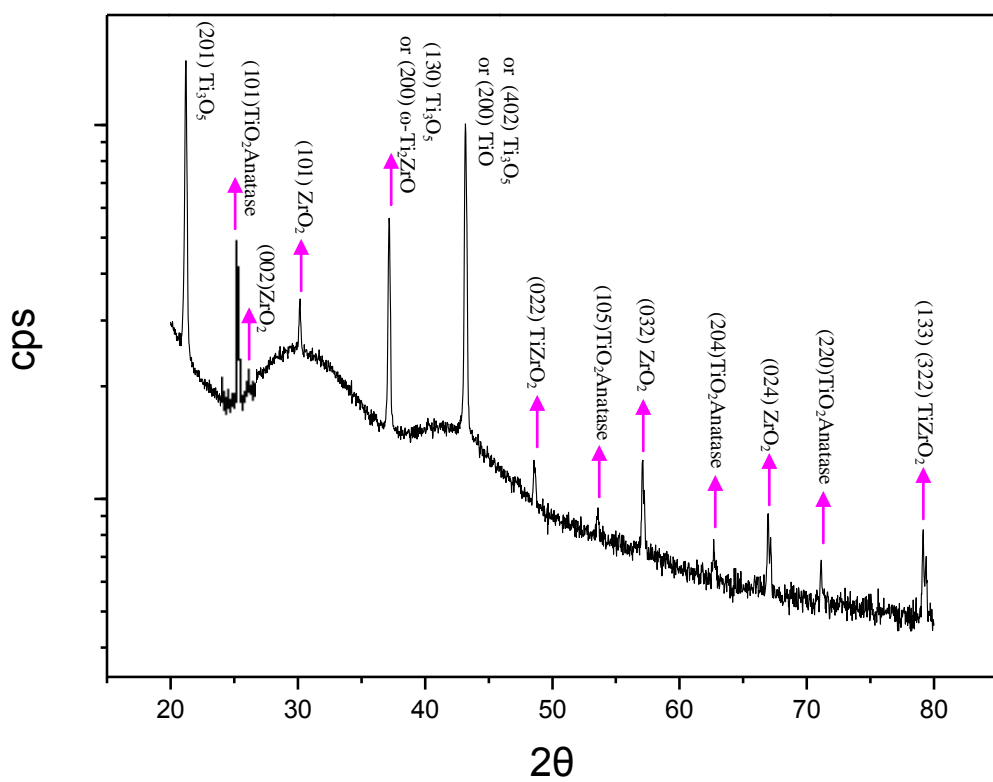
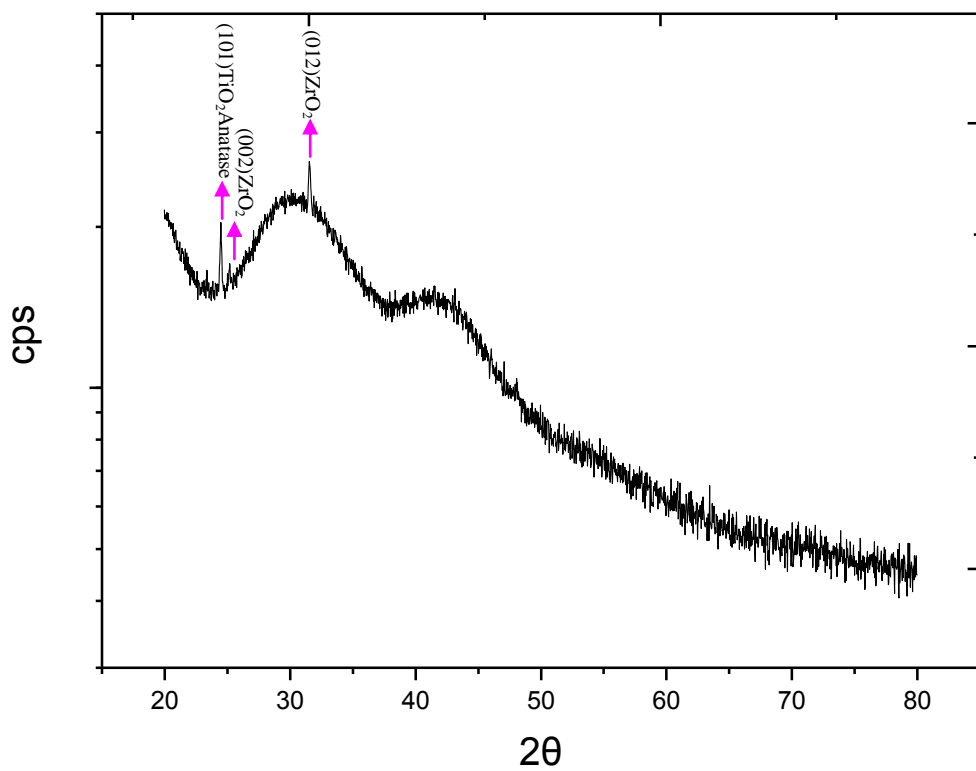
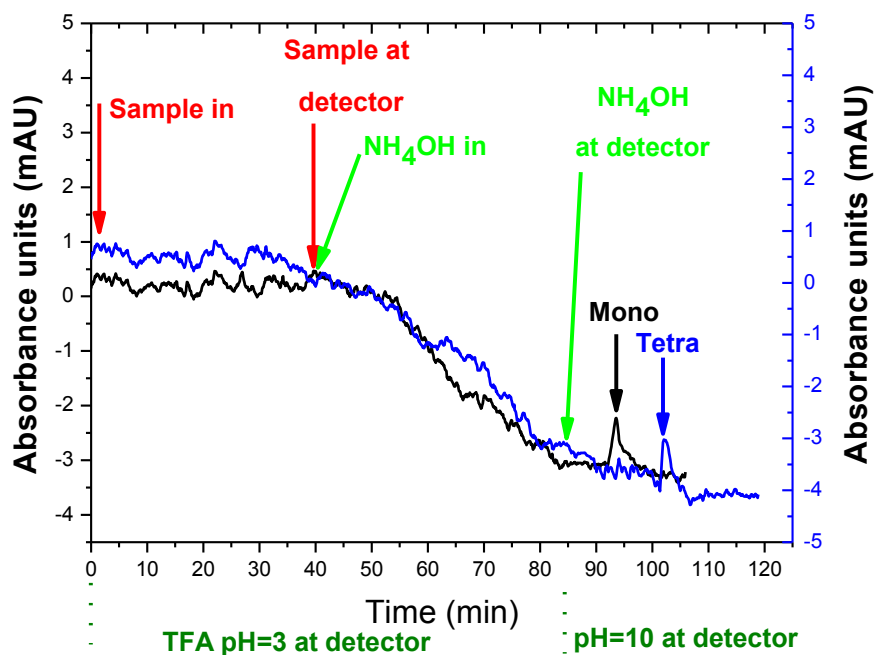


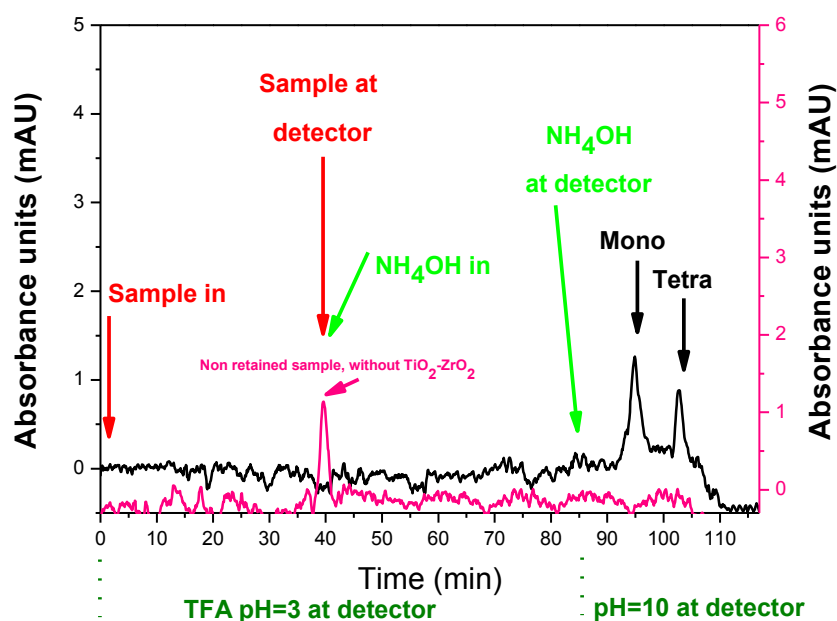
**Fig. S2** XRD spectrum after the liquid phase deposition of (a) ~80 nm and (b)~ 2400 nm  $\text{TiO}_2\text{-ZrO}_2$  film after 30 min and 16 h deposition, respectively on open PMMA surface treated in  $\text{O}_2$  plasma under the same conditions as the microchannels.

## 5. Chromatography using TFA mobile phase

The elution of mono-phosphopeptide occurred at approximately 9 min and of tetra-phosphopeptide at 17 min after the basic phase reached the detector (see Fig. S3 (a)). Effective was also the separation of the mixture, where the elution of mono-phosphopeptide occurred at 9.1 min and of tetra-phosphopeptide at 17.1 min (see Fig. S3 (b)).



(a)

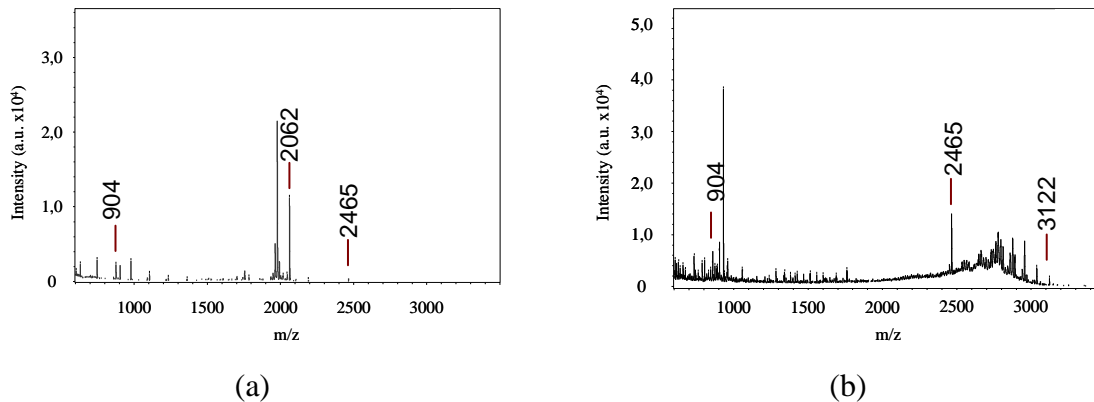


(b)

**Fig. S3** Affinity chromatography on chip, with retention, elution and separation (a) of monophosphopeptide (FQ-pS-EEQQQTEDELQDK) and tetraphosphopeptide (RELEELNVPGEIVEpSLpSpSpSEESITR), and (b) of their mixture using a PMMA micro-column containing a liquid deposited TiO<sub>2</sub>-ZrO<sub>2</sub> stationary phase. The acidic mobile phase (pH 3) was trifluoroacetic acid 0.05%, while the basic mobile phase was aqueous NH<sub>4</sub>OH (pH 10). Fig. S3 (b) also show the non-retained mixture sample in a column without TiO<sub>2</sub>-ZrO<sub>2</sub> film. The sample quantity was 4 μL (50 μM), i.e. 0.2 nmol ~ 0.4 μg for mono-phosphopeptide and ~ 0.6 μg for tetra-phosphopeptide, and the flow rate of the mobile phase was 2 μL/min. Some baseline shifts are due to shifting of the intensity of the Deuterium lamp.

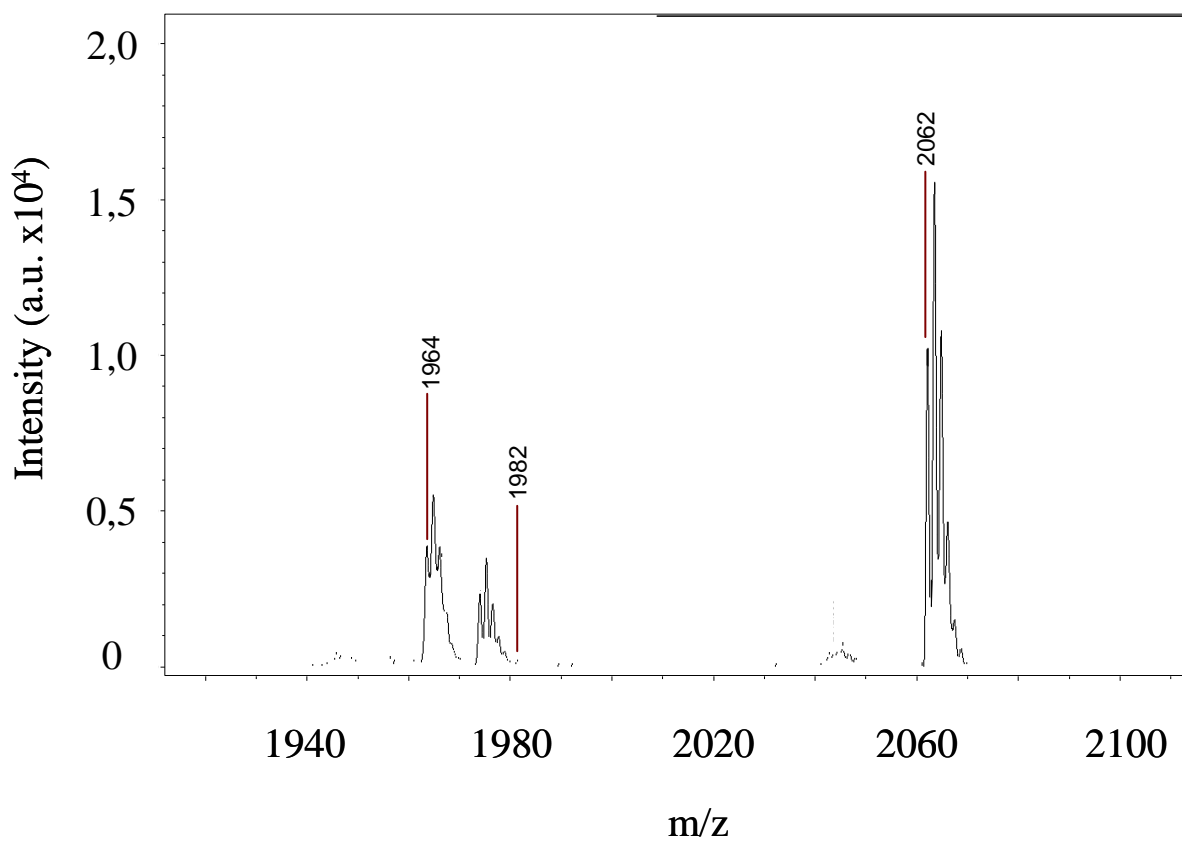
## 6. MALDI spectra of prototype phosphopeptides as purchased

Fig. S4 (a, b) presents MALDI MS spectra obtained from standard mono- and tetra- phosphopeptides before the use of the microcolumn. The peptide purity was >95% and a number of non-phosphorylated peptides were observed together with the phosphorylated peptides possibly corresponding to contaminants of the peptide standards.

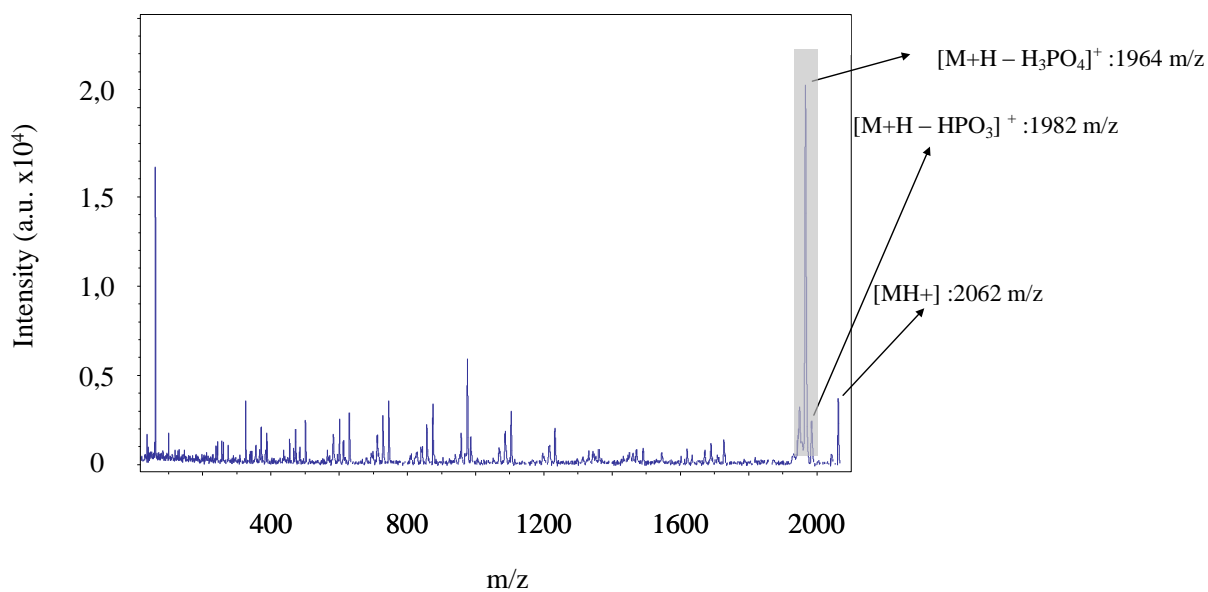


**Fig. S4** MALDI-MS spectra of (a) mono and (b) tetra phosphopeptides as purchased and dissolved in TFA solution at a concentration of 50 μM before using the microcolumn: peaks at m/z 2062 and at m/z 3122 correspond to the mono and tetra phosphopeptides, respectively; Peaks at m/z 904 and m/z 2465 correspond to the bradykinin and ACTH internal calibration standards.

Fig. S5 (a, b) corresponds to the monophosphopeptide signal response at  $m/z$  2062, and the post source decay (PSD) signal response at  $m/z$  1982 and  $m/z$  1964 that most likely occurred within the flight tube from the loss of the  $-\text{HPO}_3$  and  $-\text{H}_3\text{PO}_4$  moieties. The lack of expected mass resolution for the isotope signal response at  $m/z$  1982 and  $m/z$  1964 was indicative for this PSD. The relative intensities are coherent with the abundance of the fragmentation  $-\text{H}_3\text{PO}_4 \gg -\text{HPO}_3$ .



(a)



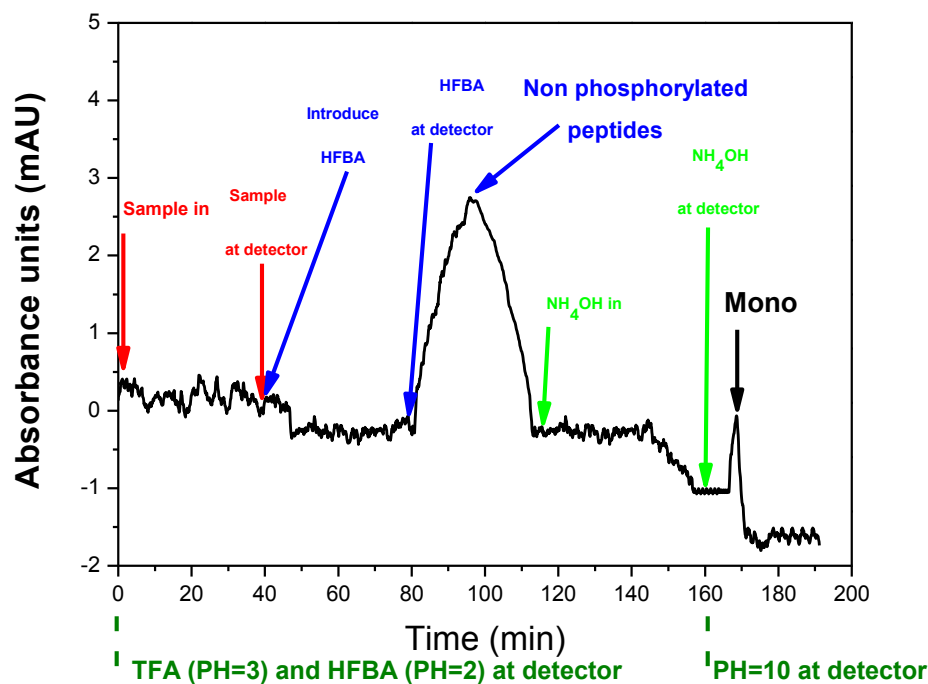
(b)

**Fig. S5** (a) Lift MS/MS spectrum before fragmentation zoomed in the  $m/z$  region 1900-2100. (b) Lift MS/MS spectrum of the peak at  $m/z$  2062 corresponding to the standard monophosphopeptide. The MS/MS precursor and product ion spectrum due to PSD or metastable decay are shown. The loss of phosphoric acid by metastable fragmentation is marked with a gray box.

## 7. Separation of phosphopeptides from Tryptone enzymatic digest from $\beta$ -Casein

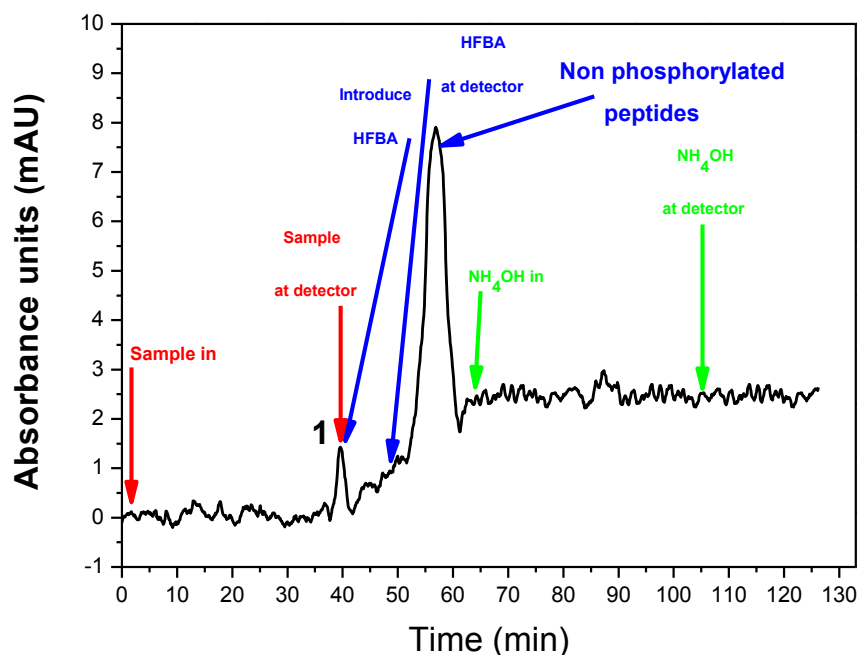
Fig. S6 shows the chromatographic separation of  $\beta$ -Casein at  $41\mu\text{M}$  concentration,  $4\mu\text{L}$  volume using as mobile phase 0.05% TFA at a flow rate of  $2\mu\text{L}/\text{min}$  on the chip containing the  $\text{TiO}_2\text{-ZrO}_2$  stationary phase. We observe that the phosphopeptides passed through the column and were retained, confirming the ability of the  $\text{TiO}_2\text{-ZrO}_2$  column to trap the phosphopeptides from the complex peptide mixture. On the contrary, in the null column we see the breakthrough of the phosphopeptide when the stationary phase is absent. We then switched the mobile phase from TFA to HFBA 0.1% (pH 1) with a flow rate of  $2\mu\text{L}/\text{min}$  in order to remove other acidic non-phosphorylated peptides from the column. At time  $t = 80$  min, HFBA reached the detector and the effectiveness of HFBA in the removal of non-phosphorylated peptides was recorded as a large peak of peptides shown in the chromatogram. Then, by introducing  $\text{NH}_4\text{OH}$ , the mono-phosphopeptide was successfully eluted 9-10 min after  $\text{NH}_4\text{OH}$  reached the detector. The elution time matches the elution time of the standard mono-phosphopeptide, although co-elution of other remaining acidic peptides cannot be excluded.





**Fig. S6** Chromatographic separation of 4  $\mu\text{L}$   $\beta$ -Casein tryptic digest at 41  $\mu\text{M}$  concentration, using the same PMMA micro-column (as in Fig. S3) with  $\text{TiO}_2\text{-ZrO}_2$  deposited stationary phase. The acidic mobile phase was TFA 0.05% (PH 3), the highly acidic phase for the removal of non-phosphorylated peptides was HFBA 0.1% (pH 1), and the basic mobile phase was  $\text{NH}_4\text{OH}$  (PH 10). The curve shows: Sample introduction, change of mobile phase from TFA to HFBA, elution of non-phosphorylated peptides, change from HFBA to  $\text{NH}_4\text{OH}$  phase, elution of phosphopeptide.

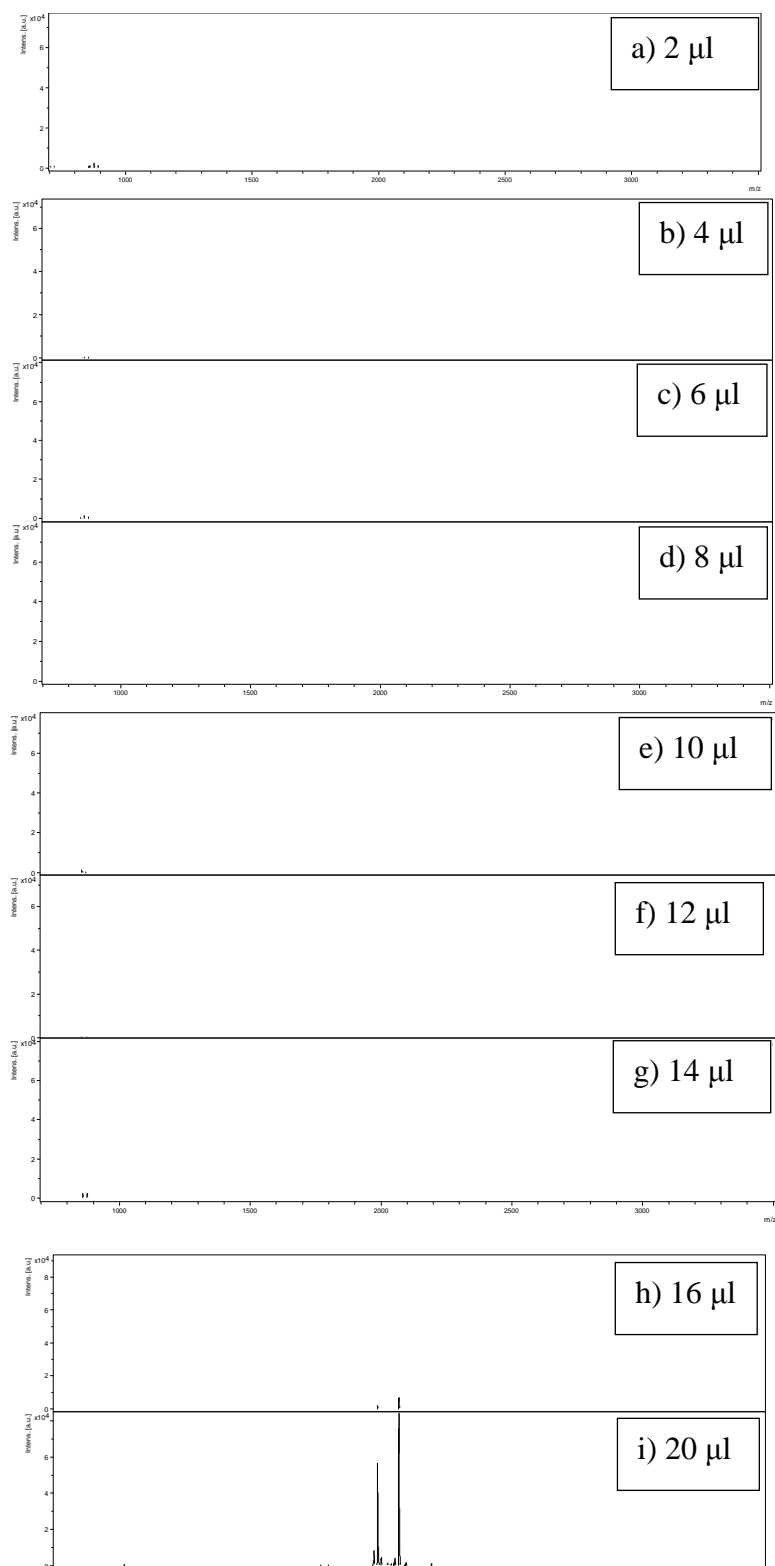
A chromatogram in a null column lacking stationary phase shows that the phosphopeptide can not be retained in this case. At a RT of 40 min, breakthrough of phosphopeptides was observed from the  $\text{TiO}_2\text{-ZrO}_2$  null chip when using the acidic mobile phase, as shown in Fig. S7. Then with the introduction of HFBA 0.1% a large peak is observed. Clearly, the rough, high-surface-area PMMA column retains non-phosphorylated peptides which are eluted with strong acid. Finally, with the introduction of the basic  $\text{NH}_4\text{OH}$  mobile phase, no peak can be observed in the chromatogram, confirming that the phosphopeptides were not trapped in the column lacking the stationary phase.



*Fig. S7 The same experiment as in Fig. S5 in a null column lacking stationary phase shows that the phosphopeptide can not be retained in this case. (Note that after observing the first peak at  $t=45\text{min}$  the flowrate was increased to accelerate the experiment)*

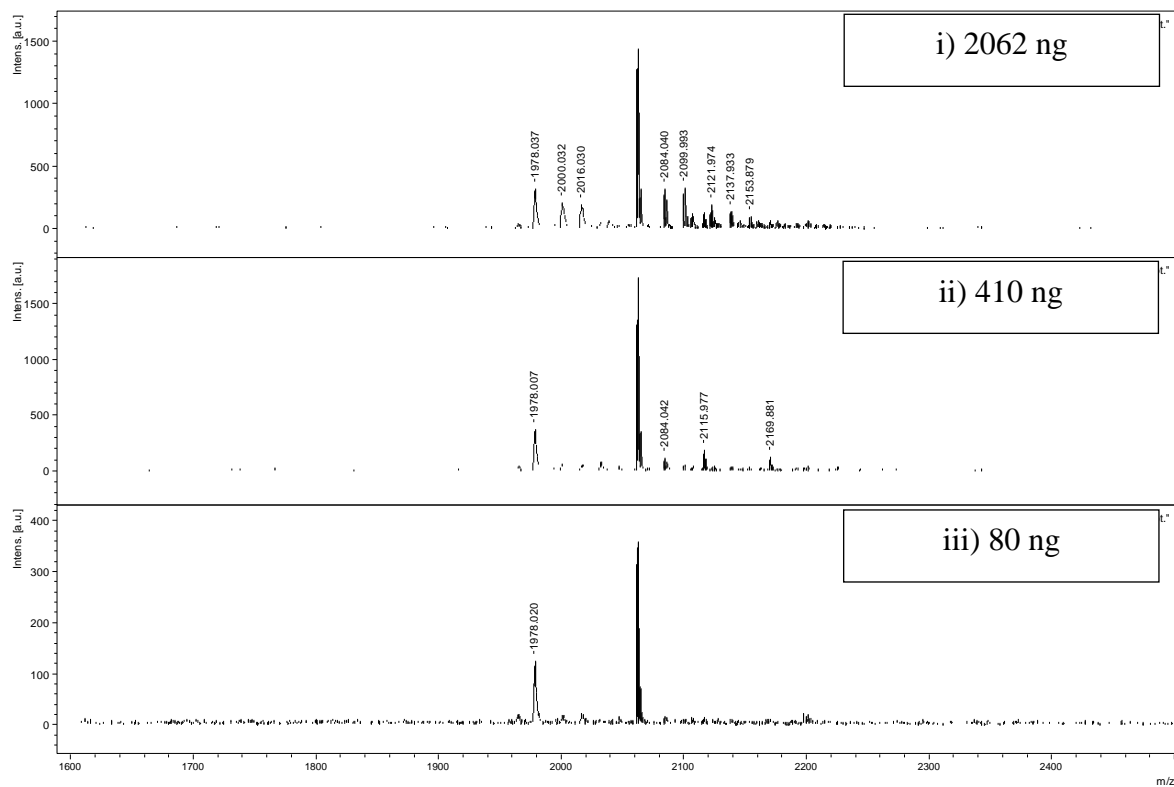
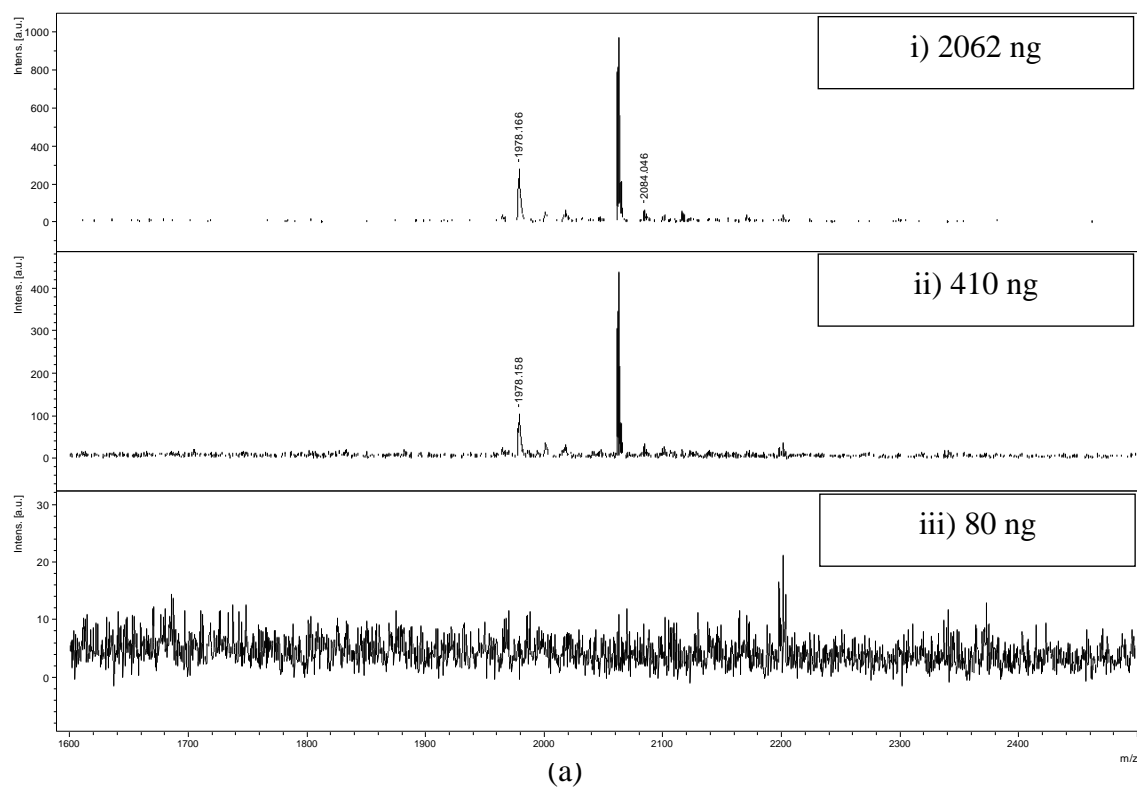
## 8. Column capacity confirmed by MALDI MS

Fig. S8 (a-1) shows the MS spectra of the effluents of all the injections collected after 40min, the time a breakthrough would be seen if the phosphopeptides were not retained. The spectra show that there was no breakthrough of phosphopeptides eluting until the quantity 14  $\mu\text{L}$ , 50  $\mu\text{M}$ , confirming that the micro-column capacity was larger than  $\sim 0.7\text{ nmol}$ ,  $\sim 1.4\text{ }\mu\text{g}$ .



**Fig. S8** (a-i) MALDI MS spectra obtained from prototype mono-phosphopeptide effluents to confirm retention in the column. Effluents of different injections after 40min using TFA 0.05%. Notice that there is no breakthrough until the 14  $\mu$ L, 50  $\mu$ M.

Experiment with commercially available tips, porous titanium dioxide Gel-Loader NuTips™ (product no. GT1TIO), from Glygen Corp. (Columbia, MD, USA). Fig. S9 (a, b) shows the MS spectra of the effluents after the (a) wash step with 0.1 % TFA and after the (b) elution with NH<sub>4</sub>OH (pH 10).



*Fig. S9 (a, b) MS spectra of the effluents porous titanium dioxide Gel-Loader NuTips<sup>TM</sup> after the (a) wash step with 0.1 % TFA and after the (b) elution with NH<sub>4</sub>OH (pH 10)*